





## Original Article

## Linking brain structure, cognition, and sleep: insights from clinical data

Ruoqi Wei<sup>1,2,3,4,†</sup>, Wolfgang Ganglberger<sup>2,3,5,6,†</sup>, Haoqi Sun<sup>2,3,5</sup>, Peter N. Hadar<sup>7</sup>, Randy L. Gollub<sup>8,9,10</sup>, Steve Pieper<sup>11</sup>, Benjamin Billot<sup>12</sup>, Rhoda Au<sup>13</sup>, Juan Eugenio Iglesias<sup>9,10,12,14</sup>, Sydney S. Cash<sup>7</sup>, Soriul Kim<sup>15</sup>, Chol Shin<sup>15,16</sup>, M. Brandon Westover<sup>2,3,5,\*</sup> and Robert Joseph Thomas<sup>1,3,10,\*</sup>

<sup>1</sup>Division of Pulmonary Critical Care & Sleep Medicine, Department of Medicine, Beth Israel Deaconess Medical Center, Boston, MA, USA

<sup>2</sup>McCance Center for Brain Health, Massachusetts General Hospital, Boston, MA, USA

<sup>3</sup>Division of Sleep Medicine, Harvard Medical School, Boston, Massachusetts, USA

<sup>4</sup>Department of Health Outcomes and Biomedical Informatics, College of Medicine, University of Florida, Gainesville, FL, USA

<sup>5</sup>Department of Neurology, Beth Israel Deaconess Medical Center, Boston, MA, USA

<sup>6</sup>Sleep and Health Zurich, University of Zurich, Zurich, Switzerland

<sup>7</sup>Department of Neurology, Massachusetts General Hospital, Boston, MA, USA

<sup>8</sup>Department of Psychiatry, Massachusetts General Hospital, Boston, MA, USA

<sup>9</sup>Department of Radiology, Massachusetts General Hospital, Boston, MA, USA

<sup>10</sup>Athinoula A. Martinos Center for Biomedical Imaging, Massachusetts General Hospital, Boston, MA, USA

<sup>11</sup>Isomics, Inc. Cambridge, MA, USA

<sup>12</sup>Computer Science and Artificial Intelligence Lab, MIT, Boston, MA, USA

<sup>13</sup>Anatomy & Neurobiology, Neurology, Medicine and Epidemiology, Boston University Chobanian & Avedisian School of Medicine and School of Public Health, Boston University, Boston, MA, USA

<sup>14</sup>Center for Medical Image Computing, University College London, London, UK

<sup>15</sup>Institute of Human Genomic Study, College of Medicine, Korea University, Seoul, Republic of Korea

<sup>16</sup>Biomedical Research Center, Korea University Ansan Hospital, Ansan, Republic of Korea

<sup>†</sup>These authors contributed equally to this work.

\*Corresponding author. Robert Joseph Thomas, Beth Israel Deaconess Medical Center, Boston, MA 02215, USA. Email [rthomas1@bidmc.harvard.edu](mailto:rthomas1@bidmc.harvard.edu); Corresponding author. M. Brandon Westover, Beth Israel Deaconess Medical Center, Boston, MA 02215, USA. Email [bwestove@bidmc.harvard.edu](mailto:bwestove@bidmc.harvard.edu).

## Abstract

**Study Objectives:** To use relatively noisy routinely collected clinical data (brain magnetic resonance imaging (MRI) data, clinical polysomnography (PSG) recordings, and neuropsychological testing), to investigate hypothesis-driven and data-driven relationships between brain physiology, structure, and cognition.

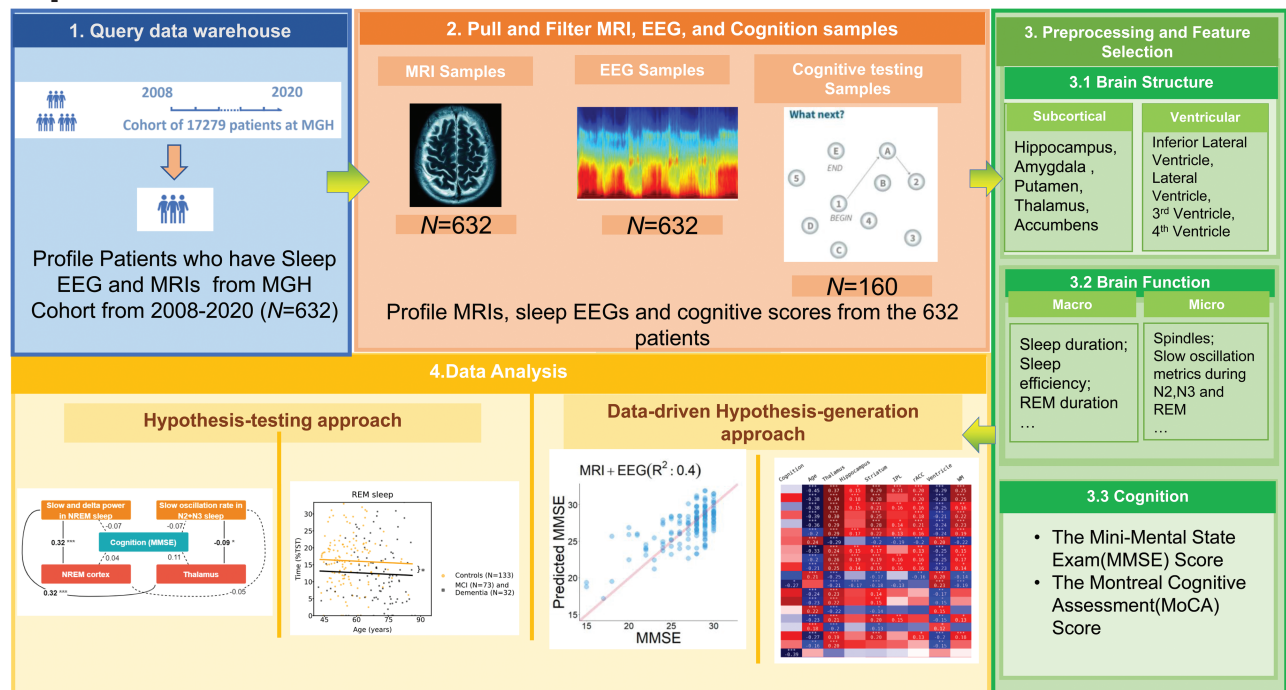
**Methods:** We analyzed data from patients with clinical PSG, brain MRI, and neuropsychological evaluations. SynthSeg, a neural network-based tool, provided high-quality segmentations despite noise. A priori hypotheses explored associations between brain function (measured by PSG) and brain structure (measured by MRI). Associations with cognitive scores and dementia status were studied. An exploratory data-driven approach investigated age-structure-physiology-cognition links.

**Results:** Six hundred and twenty-three patients with sleep PSG and brain MRI data were included in this study; 160 with cognitive evaluations. Three hundred and forty-two participants (55%) were female, and age interquartile range was 52 to 69 years. Thirty-six individuals were diagnosed with dementia, 71 with mild cognitive impairment, and 326 with major depression. One hundred and fifteen individuals were evaluated for insomnia and 138 participants had an apnea-hypopnea index equal to or greater than 15. Total PSG delta power correlated positively with frontal lobe/thalamic volumes, and sleep spindle density with thalamic volume. rapid eye movement (REM) duration and amygdala volume were positively associated with cognition. Patients with dementia showed significant differences in five brain structure volumes. REM duration, spindle, and slow-oscillation features had strong associations with cognition and brain structure volumes. PSG and MRI features in combination predicted chronological age ( $R^2 = 0.67$ ) and cognition ( $R^2 = 0.40$ ).

**Conclusions:** Routine clinical data holds extended value in understanding and even clinically using brain-sleep-cognition relationships.

**Key words:** cognition; sleep; brain health; polysomnography; electroencephalography; magnetic resonance imaging

## Graphical Abstract



## Statement of Significance

Our study has validated previous hypotheses about sleep-brain structure associations using routine clinical data and introduced the concept that data-driven selection of EEG and magnetic resonance imaging (MRI) features could significantly enhance predictions of cognitive status and age. This highlights the potential role of multivariable analytics in clinical practice, providing a pathway to expand the utilization of clinical EEG and structural MRI data in future studies and clinical applications. Our findings underscore the importance of an integrated, holistic view of the relationship between sleep, brain structure, and cognition, offering the potential for a more comprehensive understanding of neurological and psychological disorders and potentially improving patient care. Furthermore, the ability to extract valuable information from routine clinical data, such as polysomnography and MRI, suggests the possibility of identifying brain health risks, disease progression, and the evaluation of therapeutic interventions in a clinical setting. This study represents a step towards harnessing the full potential of clinical data to benefit patients and advance our understanding of the complex interplay between sleep, brain health, and cognition.

## Introduction

rapid eye movement (REM) sleep [1–5] and non-REM sleep [6–9] have distinct oscillations within distinct frequency ranges. Some of the brain origins of these oscillations are known and relatively localized, such as the reticular thalamic-thalamocortical relay for sleep spindles [10], while slow waves have more distributed generators from anterior and medial cortical areas [11–13]. The fast oscillations typical of REM sleep originate from brain-activating sites but project diffusely. It is thus to be expected that disease states that impact brain networks should alter these sleep oscillations, and it may be possible to read out sleep-brain oscillations to detect disease at various stages of evolution [14–18].

There are systematic changes in sleep macro [19–26] and micro [8, 27] architecture associated with the aging process regardless of the presence of disorders such as sleep apnea and periodic limb movement disorder. There is a reduction in slow waves and thus deep sleep (non-REM stage 3), sleep spindles and K-complexes, total sleep time (TST) and sleep efficiency [28], a mild reduction in REM sleep, and an increase in arousals and light sleep (non-REM stage 1) [29]. With increasing age, sleep becomes briefer, more fragmented, and has less REM and deep non-REM sleep [30, 31].

Older brains exhibit decreased alpha oscillations while awake; and in sleep, less slow wave activity [32–34], spindle amplitude, and density [27], and slow wave/spindle coupling [8].

All of these changes are amplified by Alzheimer's disease (AD) and related dementias, as well as non-AD neurodegenerative disease [35, 36]. In addition, specific cognitive deficits are associated with pathology of specific sleep oscillations generated by specific brain structures, e.g. reduced sleep spindles and hippocampal atrophy [8, 37, 38], and age-related memory impairment [39, 40]. Considering the evidence from numerous studies highlighting the crucial role of sleep in supporting cognitive processes [41–45], it is increasingly apparent that there may be a connection between changes in sleep patterns and the accelerated cognitive decline and impairment observed in older adults [46–50]. Indeed, as the brain networks generating sleep oscillations are the same networks engaged in cognitive processes, analysis of sleep may also allow prediction of impaired cognition [51–53].

Questions regarding the specific brain structural abnormalities that might influence sleep patterns and quality [54–56], the extent to which good sleep quality can compensate for neuropathology [57], and the compensatory role of healthy brain structure in the

presence of sleep pathology [58] are actively being investigated. Notably, certain studies suggest that individuals with resilient brain structures may exhibit better sleep quality even in the presence of sleep disorders or disruption [59]. Emerging work also suggests that the sleep state encodes information about brain health [60, 61], not evident in standard stages and similar metrics.

Structural magnetic resonance imaging (MRI) of the brain is a frequent clinical examination for diverse reasons. Typically, once the clinical question is answered (e.g. —is there a brain tumor?), the rest of the data are effectively discarded (euphemistically, “archived”). Extracting regional brain volumes is generally considered difficult, and the focus of clinical imaging is on detecting discrete pathology [62]. Similarly, clinical PSG usually reports the apnea–hypopnea index and sleep stages, discarding the majority of the information content of hours-long recordings. Can MRI and PSG data be put to better use? Most clinical PSG is actually research standard/quality data, based on standards of the American Academy of Sleep Medicine; and extracting sleep power bands and spindle kinetics, as examples, is readily achieved even if not done in clinical care. This is not true for MRI, with a wide variety of scan parameters including resolution. SynthSeg is a recently developed convolutional neural network-based segmentation tool that is compatible with clinical-grade brain MRI scans of widely varying contrast and resolution without retraining or fine-tuning. SynthSeg\* includes an option to increase the robustness of the segmentation process and to facilitate the synthesis of higher-resolution images derived from lower-resolution scans, even when there are variations in orientation, resolution, and MRI contrast [63, 64]. SynthSeg\* can be used across a wide array of participant populations from young and healthy to aging and diseased participants, with or without preprocessing (bias field corruption, skull stripping, intensity normalization, and registration to template). Importantly, the output segmentations are returned at high resolution (1 mm isotropic) regardless of the resolution of the input scans. This presents an opportunity to align MRI and PSG as never before to probe brain structure–function relationships in health and disease.

Herein we first tested the hypotheses that (1) sleep spindles/sigma power are associated with thalamic volumes, and spindle abnormalities are associated with memory deficits and hippocampal atrophy [8, 37, 38], (2) sleep slow wave/delta power is associated with cortical volumes, and a reduction is associated with impaired cognition [65–67], (3) specific sleep macro and microstructure are associated with specific brain volumes and cognition [68–70], and (4) the combination of sleep electroencephalogram (EEG) from PSG and brain MRI data are better predictors of cognition than either assessment alone [71–73]. We then employed a data-driven discovery approach to investigate how much of the variation in measures of sleep, brain structure, cognition, and presence of dementia are explained by regression models based on hypothesis-based relationships alone compared with data-driven models. In the process, we identified potential novel structure–function–behavior associations, and gained insights into how much information each modality provides about the others. Importantly, our input data used clinical MRIs across a heterogeneous group of patients who also underwent clinically indicated polysomnograms and basic cognitive testing with the Mini-Mental State Examination (MMSE) and/or Montreal Cognitive Assessment (MoCA). We used machine learning approaches to probe sleep-related brain oscillations and assessed three-way associations and predictions with brain structure and cognition.

## Methods

The study procedures were approved by the Mass General Brigham Institutional Review Board. Due to the deidentification of the data used in this retrospective data analysis, the requirement for individual-level informed consent was waived. This study adheres to the Strengthening the Reporting of Observational Studies in Epidemiology (STROBE) reporting guidelines, ensuring comprehensive and transparent reporting of the study methodology and results.

## Study cohort

This cross-sectional analysis used a convenience dataset comprised of patients who underwent both clinical PSG and clinical brain MRI at the Massachusetts General Hospital, with the two studies per patient acquired within a 5-year interval, all studies completed between 2008 and 2020. Participants were required to meet the following inclusion criteria: (1) age between 18 and 80 years, and (2) underwent full night diagnostic PSG (not a split night study). Age in this study was determined as age at the time of the sleep polysomnography.

## MRI data

MRI data closest to the date of the PSG that included a whole brain volume of T1, T2, fluid-attenuated inversion recovery (FLAIR), or diffusion sequence was selected for analysis if there were multiple scans for a patient. SynthSeg\* [63, 64] based on FreeSurfer (Version v7.3.2) [74], neuroimaging software were used, together with custom processing scripts and tools for facilitating quality control review. SynthSeg, a recent convolutional neural network-based tool, is designed for segmenting brain regions in clinical-grade MRI scans, accommodating varying contrasts and resolutions. This tool enhances segmentation robustness and can generate high-resolution images (1 mm isotropic) from lower-resolution scans, even amidst variations in orientation and MRI contrast. It was designed to be versatile, suitable for a broad spectrum of participants, from young and healthy to aging and diseased. Notably, the output remains at a high resolution, irrespective of the input scan’s resolution. We used SynthSeg to automatically segment various brain regions from clinical MRI sequences, resulting in 94 regional cortical and subcortical volume measures for each hemisphere. The raw MRI images and the SynthSeg processing outputs were reviewed manually by two physician-scientists (RG, PH) with expertise in neuroanatomy to ensure that all derived measures came from whole brain images (no partial volumes) and to exclude cases with strokes, neoplasms, traumatic injury, and other structural lesions that corrupted the automated volumetric data. In datasets with multiple acquisition sequences passing this quality control, the order of preferred selection was T1, T2, FLAIR, then Diffusion-Weighted, to achieve the most accurate assessment [63, 64]. We summed left and right hemisphere volumes, and to account for inter-participant anatomical differences, all MRI regional volume measures were normalized by the individual’s total intracranial volume (ICV) [75, 76] using the division method, i.e. calculating the ratio between the volumes of interest and the total ICV, generating a unitless value ranging from 0 to 1.

## Sleep EEG data

EEG signals were recorded at a minimum sampling rate of 200 Hz and segmented into non-overlapping 30-second epochs. These epochs were manually scored by certified sleep technicians following the standards set by the American Academy of Sleep

Medicine [77] as part of routine clinical care. The EEG signals consisted of six channels: frontal (F3-M2 and F4-M1), central (C3-M2 and C4-M1), and occipital (O1-M2 and O2-M1), each reference to the contralateral mastoid. The scored epochs were categorized into one of the five sleep stages: wake (W), REM, non-REM stage 1 (N1), Non-REM stage 2 (N2), and Non-REM stage 3 (N3). These clinical studies were reported after epoch-by-epoch review by Board Certified Sleep Medicine specialists, thus providing a layer of quality control.

To minimize non-physiological artifacts, the EEG signals were notch-filtered at 60 Hz to reduce line noise and bandpass filtered from 0.3 Hz to 50 Hz. For the 30-second epochs, those with an absolute amplitude larger than 500  $\mu$ V were removed from analysis to mitigate movement artifacts. Additionally, epochs containing flat EEG for more than 2 seconds were excluded. From the hypnograms, 20 macro-structure architecture features were derived, including total resting time, TST, durations of each sleep stage, percentage of time spent in each sleep stage, sleep efficiency index (calculated as TST divided by total resting time), sleep onset latency (time to the first sleep stage), time to first awake period after sleep onset (WASO), REM latency, number of stage shifts to Wake from NREM/REM sleep (NA), number of stage shifts to N1 from NREM/REM sleep (NSS), and sleep fragmentation index ([78], calculated as [NA + NSS] divided by TST).

For each 30-second epoch and EEG channel, EEG microstructure data were extracted using similar features as those used in previous work for sleep staging [79]. In total, 1054 microstructure features were extracted from the full night of recording. Specifically, we extracted features from 2-second windows with step sizes of one second for each 30-second epoch, covering both time and frequency domains. In the time domain, we considered features such as line length, kurtosis, and sample entropy. In the frequency domain, we analyzed features such as the 95th percentile, minimum, mean, and standard deviation of relative delta/theta/alpha band power. Additionally, we examined the 95th percentile, minimum, mean, and standard deviation of the delta-theta/delta-alpha/theta-alpha power ratio, as well as the kurtosis of the delta/theta/alpha/sigma band spectrogram. For each EEG recording, we calculated the average of these features within each of the five sleep stages over time, resulting in 1054 features per EEG. To better characterize NREM sleep homeostasis, we quantified the total delta power (<4Hz) during N2 and N3 sleep stages for the entire sleep duration, the initial 4 hours, and up to the first REM episode. We further applied linear regression to the epoch-wise < 4Hz power data in N2 and N3, extracting both intercept and slope. For REM characterization, we calculated the total power in delta, theta, and alpha frequency bands for the first REM episode and all subsequent REM episodes. Additionally, we computed a total of 93 spindle and slow-oscillation (SO) features with Luna software [80]. Spindle features were extracted in N2 sleep with central frequencies of 11.5 Hz (referred to as “slow spindles”) and 15.5 Hz (referred to as “fast spindles”) from the frontal, central and occipital channels. SO and SO-spindle coupling features were extracted in N2 and N3 stages. To streamline the analysis, we performed feature reduction by eliminating highly correlated features. Features with a Pearson correlation coefficient greater than 0.95 were deemed highly correlated and thus were eliminated from the analysis. This step reduced the total number of features from 1167 to 776. To ensure approximate Gaussian distributions, we applied a logarithmic transformation to the features. Subsequently, we standardized the features using z-transformation, which involved adjusting them to have a mean of zero and a standard deviation of one in the training set. The same z-transformation was also applied to

the testing set. Furthermore, we employed a data-driven approach and predefined restrictions to group the sleep EEG features. The sleep feature supergroups were categorized as wake and N1 stages combined (“W+N1”), N2 and N3 stages combined (“N2+N3”), REM sleep (“REM”), and macro features (“Macro”). Subsequently, features within these supergroups were clustered into subgroups or “clusters” based on their correlation matrices. Ward’s algorithm [81] was employed for clustering, using Euclidean distance as the distance metric. Upon manual inspection, we selected a maximum distance of 12 within clusters. Cluster metrics are reported in the supplement.

## Cognitive and health data

In prior work from our group [82], we developed a method to extract cognition-related information from electronic medical records. Scores for the MMSE and MoCA, and diagnoses for mild cognitive impairment (MCI) and dementia, when available, were extracted from clinical notes using regular expressions. These examinations were conducted as part of clinical care, primarily within neuropsychiatric evaluations, to assess cognitive problems. For the present study, we manually reviewed clinical notes to confirm or correct MMSE and MoCA scores, as well as MCI and dementia diagnoses. To achieve compatibility across scores, we converted MoCA scores to equivalent MMSE scores using an equipercentile equating method as previously described [83].

We further extracted ICD-10 codes at the time of the sleep studies, and computed the overall Charlson comorbidity index and, based on Elixhauser Comorbidity methodology, categorized participants into additional, non-exclusive disease categories: myocardial infarction, congestive heart failure, peripheral vascular disease, cerebrovascular disease, chronic pulmonary disease, rheumatoid disease, peptic ulcer disease, mild liver disease, diabetes without complications, diabetes with complications, hemiplegia or paraplegia, renal disease, cancer (any malignancy), moderate or severe liver disease, metastatic solid tumor, AIDS/HIV, alcohol abuse, drug abuse, psychoses, and depression. We report the prevalence of these comorbidities as part of the baseline demographic information (see Table 1). Furthermore, the most prevalent diseases in our cohort (dementia, MCI, depression, cancer, diabetes, congestive heart failure, peripheral vascular disease, and cerebrovascular disease) were used for sensitivity analyses (detailed below). Here, dementia and MCI were treated as mutually exclusive from other disease groups. Participants without dementia or MCI could belong to multiple disease groups. This approach was taken to ensure that the influences of neurodegenerative dementia diseases on brain structure and function did not overly confound results for other disease groups.

## Statistical analyses

All statistical tests used in this study were two-sided unless noted otherwise. We employed Python (3.11.3) and R (4.3.1) statistical software for the analysis. Only data within a time interval of 5 years between PSG, MRI, and cognitive scores were included for analysis. To ensure the reliability of the data, patients with cognitive decline due to stroke, Parkinson’s disease, mental illness, vascular dementia, Lewy body dementia, brain tumor, and paraneoplastic syndrome were identified and excluded. This was done by manually reviewing MRI images and clinical notes. Additionally, to minimize the risk of spurious associations between MRI, PSG, and cognitive scores, all patients’ clinical reasons for visits and corresponding visit dates were carefully examined in the PSG reports, MRI reports, and cognitive reports. In cases where a

**Table 1.** Demographic and Baseline Clinical Information

<b>N participants with PSG and MRI</b>	<b>632</b>	<b>160</b>
Age: year, median (IQR)	61 (52, 69)	67 (58, 73)
Age: number (%)		
	<20	0 (0)
	20–40	34 (6)
	40–60	248 (40)
	60–80	306 (49)
	>80	34 (6)
Sex: number (%)		
	Female	342 (55)
	Male	281 (45)
Race		
	White	522 (84)
	Black	43 (7)
	Asian	8 (1)
	American/Alaska	3 (0)
	Other	31 (5)
	Unavailable	15 (2)
Ethnicity		
	Hispanic	39 (6)
	Non Hispanic	550 (88)
	Unavailable	34 (5)
N diagnostic PSG studies	632 (100)	160 (100)
Apnea–hypopnea index (3% desaturations)		
	Normal (AHI < 5)	241 (39)
	Mild (5 ≤ AHI < 15)	244 (39)
	Moderate (15 ≤ AHI < 30)	97 (16)
	Severe (30 ≤ AHI)	41 (7)
Respiratory disturbance index (RDI, events/hour) (IQR)	13 (7, 24)	12 (6, 24)
Limb movement index (events/hour) (IQR)	13 (4, 38)	17 (4, 48)
Sleep fragmentation index (IQR)	4 (3, 6)	4 (3, 6)
Epworth Sleepiness Scale (IQR)	7 (4, 11)	6 (4, 10)
Visit for insomnia evaluation: number (%)	115 (33)	27 (29)
Charlson comorbidity index (IQR)	2 (1, 3)	2 (1, 3)
	Minimal (CCI < 2)	256 (41)
	Mild (CCI == 2)	131 (21)
	Moderate (3 ≤ CCI < 5)	149 (24)
	Severe (5 ≤ CCI)	88 (14)
Diagnoses (ICD-10)	N = 583	
	Myocardial infarction	31 (5)
	Congestive heart failure	96 (17)
	Peripheral vascular disease	111 (19)
	Cerebrovascular disease	171 (29)
	Chronic pulmonary disease	217 (37)
	Rheumatoid disease	38 (7)
	Peptic ulcer disease	15 (3)
	Mild liver disease	73 (13)

Table 1. Continued

N participants with PSG and MRI	632	160
Diabetes without complications	150 (26)	31 (20)
Diabetes with complications	95 (16)	21 (14)
Hemiplegia or paraplegia	7 (1)	1 (1)
Renal disease	99 (17)	28 (18)
Cancer (any malignancy)	158 (27)	47 (30)
Moderate or severe liver disease	1 (0)	0 (0)
Metastatic solid tumor	18 (3)	3 (2)
AIDS/HIV	3 (1)	2 (1)
Alcohol abuse	37 (6)	18 (12)
Drug abuse	51 (9)	17 (11)
Psychoses	24 (4)	11 (7)
Depression	326 (56)	102 (65)
Diagnoses (chart review)		
Mild cognitive impairment	71 (11)	55 (34)
Dementia	36 (6)	23 (14)
Time between measurements (years)		
EEG—MRI	2.2 (1.9)	1.7 (1.6)
EEG—Neuropsych.	—	2.1 (2.1)
MRI—Neuropsych.	—	1.9 (2.1)

patient had multiple MRIs, PSGs, and cognitive scores, the data point closest to the median of the total time interval between them was selected.

### Part one: testing hypothesized relationships.

In the first part of this study, we tested a set of hypothesized relationships based on domain knowledge and prior literature between sleep EEG measurements (PSG), brain structural MRI, and neuropsychological MMSE scores (NP). The hypotheses were:

1. Slow oscillatory (<1 Hz) and delta (1–4 Hz) power in NREM sleep are positively associated with the volumes of the thalamus and the anterior cortex (sum of anterior cingulate cortex and medial orbitofrontal cortex), constituted by the medial orbitofrontal and the anterior cingulate cortex.
2. Slow and fast sleep spindle densities in N2 sleep positively correlate with the volumes of the thalamus and hippocampus.
3. The proportion of REM sleep is positively associated with the volumes of isthmus cingulate cortex, the amygdala, and the brainstem.
4. Alpha (8–12 Hz) power during wake correlates positively with the volumes of the thalamus and negatively with total brain ventricular volume.

Each variable was also tested for associations with cognitive performance. Pearson correlation and partial Pearson correlation, adjusted for age and sex, were used to test these associations. For every pair, we established a null hypothesis stating that no association exists between variables X and Y when controlling for age and sex. This hypothesis was rejected if the *p*-value was below 0.05. To test the robustness of these associations, we stratified the patients based on their chronological age, the time intervals between the EEG, MRI, and neuropsychological measures, as well

as disease categories. We then repeated the analysis for each of these subgroups.

We further analyzed if the variables within the a priori hypotheses differed among patients with MCI, dementia, and controls. Our non-dementia control group comprised patients who were not diagnosed with MCI or dementia and exhibited a Charlson comorbidity index of either zero or one. Considering the youngest patient in the MCI + dementia group was 42 years old, we limited the control group to individuals older than 42. We fitted individual linear regression models for each feature, where the features served as the dependent variables and age acted as the independent variable. Based on visual inspection of the data, we selected the regression models to be either first-order (linear) or second-order (quadratic). Models were established separately for controls, patients with MCI, patients with dementia, and patients with combined MCI and dementia. For age groupings divided into 5-year intervals, we calculated the 95% confidence interval of the estimated mean using bootstrapping. We determined statistical significance by examining whether or not these confidence intervals overlapped. We further performed principal component analysis incorporating all sleep and MRI features and conducted an analogous modeling process for principal components 1–4.

### Part two: exploratory analyses.

The subsequent part of our study involved exploratory analyses. These investigations sought to understand associations and predictive powers beyond the a priori hypothesized relationships between sleep, brain structure volume, and cognition. We began by determining associations via Pearson correlations between any pair of sleep-MRI, sleep-cognition, and MRI-cognition features, while controlling for multiple comparisons (see below).

Discovery of associations through block-permutation strategy: given the substantial correlations within the variables of a domain (sleep, structure), employing a Bonferroni correction

would be excessively conservative. Therefore, to tackle the issue of multiple testing and to structure the interpretation of numerous interrelated tests, we employed a block-permutation strategy to derive empirical significance values while maintaining control for multiple testing [45]. Our process involved using Omnibus permutation testing to ascertain if a feature set (for example, a sleep cluster) correlates with an independent variable (such as a specific brain structure volume, or cognition).

**Predictive modeling:** we also evaluated the variance explained for cognition and age by sleep and MRI data. Additionally, we explored the prediction of sleep features using MRI and vice versa. To mitigate the impact of a small sample size and to prevent overfitting, we employed leave-one-participant-out cross-validation (LOOCV) [84]. In LOOCV, the model is trained on all but one observation, which is used as the test set. This process is repeated for each observation, and the overall prediction performance is determined based on the test set scores only. For feature selection, we utilized the Least Absolute Shrinkage and Selection Operator penalized regularization [85], which helps identify important features and leads to simpler models. We performed hyperparameter tuning on the training set to find the optimal values that yielded the best performance. Least Absolute Shrinkage and Selection Operator conducts variable selection by shrinking the coefficients of certain variables to zero, resulting in a more interpretable and concise model. To ensure generalization of our models, we employed a strategy of hyperparameter tuning, which involved conducting a (10-1)-fold cross-validation within each iteration of the k-fold CV for classification algorithm evaluation (i.e. nested CV). This approach allowed us to fine-tune the model's parameters based on a more stable and accurate prediction performance. The (k-1) folds used in this inner cross-validation were the same as the original k-1 folds assigned for training. We evaluated the accuracy of our predictions using the Pearson's coefficient of determination ( $R^2$ ) and root mean square error (RMSE) between the measured and predicted values in all testing sets. To ensure consistency, all data were rescaled to z-scores with a mean of 0 and a standard deviation of 1. We were further interested in

assessing the difference in prediction performance if we used a priori variables only vs. all available variables as model inputs. For this purpose, we set up multiple prediction tasks: predict MMSE or age from all EEG and MRI variables versus predict MMSE or age from a priori EEG and MRI variables; predict specific brain structure volumes from all EEG variables versus predict specific brain structure volumes from a priori EEG variables only, and analogously for MRI variables. The a priori features of EEG included total slow and delta (0.4–4Hz), SO rate, slow sleep spindle density, fast sleep spindle density, percentage REM, and occipital alpha power during Wake. MRI features evaluated included volumes of the thalamus, hippocampus, isthmus cingulate, amygdala, brain stem, and total ventricles. To determine statistical significance, we evaluated if the [0, 95] and [5, 100] confidence intervals for a priori-only and full feature, respectively, overlapped. The confidence intervals were computed by bootstrapping ( $N = 10\,000$  iterations). In all of the prediction tasks, we controlled for time between EEG, MRI, and neuropsychological measures by adding the respective variables as input to the models.

## Results

Detailed data of 8673 patients who underwent polysomnography were extracted from the Sleep Laboratory of Massachusetts General Hospital. A total of 4157 MRI sessions from 632 overlapping participants were obtained, along with 467 cognition scores from 160 participants. Among the 160 patients included in the analysis, 84 had MMSE scores, and 76 had MoCA scores. See Figure 1 for consolidated standard of reporting trial (CONSORT) flow diagram and Table 1 for demographic and baseline clinical information. For the 76 patients with MoCA scores, the scores were converted to MMSE equivalent scores using the MoCA to MMSE conversion table that is commonly used for Alzheimer's disease clinical trial screening [83]. The final dataset thus consisted of 632 patients who had both PSGs and MRI and of a subset of 160 participants who additionally had MMSE equivalent scores for cognitive assessment. Histograms of the time

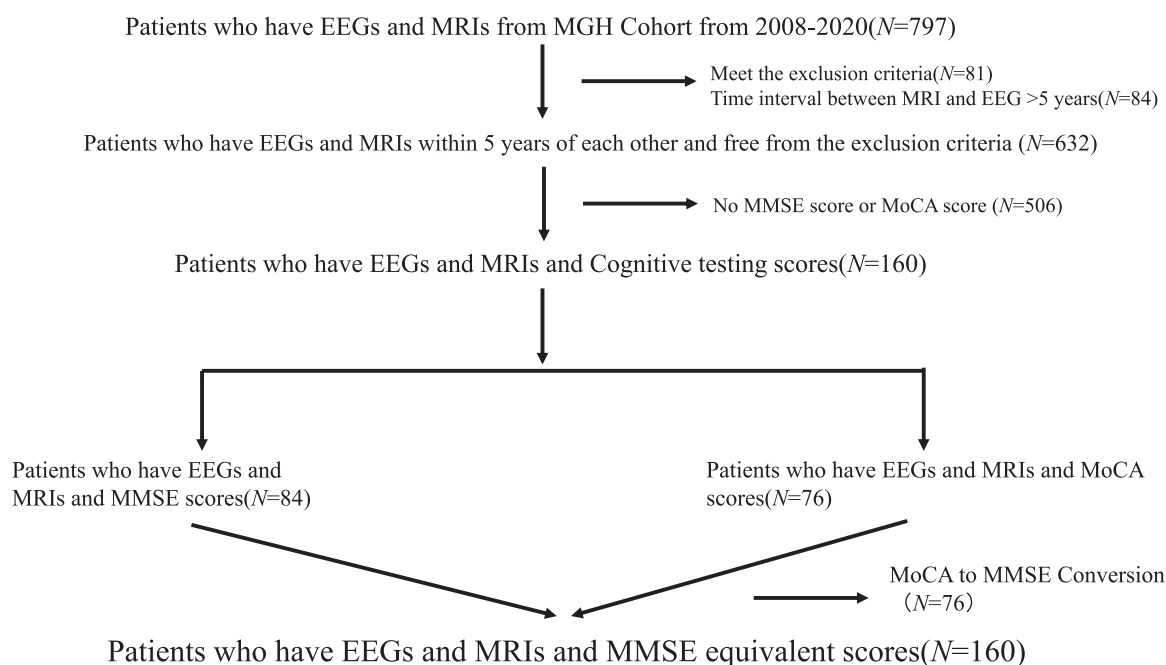


**Figure 1.** CONSORT flow diagram.

differences between different measurements are displayed in [Supplementary Figure S1](#).

The collected sample in this study was clinically diverse: 41% of participants had a Charlson Comorbidity Index score of less than two (minimal comorbidities), while 24% had a score of three or more (moderate or severe); the most common ICD-10 diagnoses were depression (56%), chronic pulmonary disease (37%) cerebrovascular disease (29%), and cancer (27%); and 11% were diagnosed with MCI and 6% with dementia. It is important to note that a single patient could have been assigned multiple ICD-10 codes if they had more than one diagnosed condition.

### Part one: testing hypothesized relationships.

The results data for the a priori hypotheses are presented in [Table 2](#), which displays both the unadjusted and the age- and sex-adjusted Pearson correlation results. Total slow and delta power (0.5–4 Hz) was significantly associated with both the volumes of anterior cortex (sum of anterior cingulate cortex and medial orbitofrontal cortex,  $r = 0.34$ ,  $p < 0.001$ ) and thalamus

( $r = 0.34$ ,  $p < 0.001$ ). Fast spindle density was associated with thalamic volume ( $r = 0.11$ ,  $p < 0.01$ ).

With two exceptions, all NREM hypotheses were confirmed in the non-adjusted version, while only the association between fast spindle density and the thalamic volume showed significance after controlling for age and sex ( $r$  unadjusted 0.31,  $r$  adjusted 0.11).

While percentage REM was not associated with the hypothesized structural volumes, both percentage REM and the amygdala volumes were associated with cognition, as measured via MMSE scores, after controlling for the covariates ( $r$  adjusted = 0.16,  $p = 0.04$ ;  $r$  adjusted = 0.20,  $p = 0.01$ , respectively). For the wake hypotheses, total ventricular volume was negatively associated with MMSE score without covariate adjustment ( $r$  unadjusted = -0.24,  $p < 0.001$ ,  $r$  adjusted = -0.15,  $p = 0.07$ ).

Sensitivity analysis of a priori hypotheses stratified by participants' chronological age and time distances between EEG, MRI, and neuropsychological measures is reported in [Supplementary Table S1](#), while stratification by disease category is reported in [Supplementary Table S2](#). Generally, the

**Table 2.** A Priori Hypotheses Between Electroencephalogram Features (Wake and Sleep), Brain Structure Volumes and Cognitive Function, as Measured by the MMSE

Feature pair	Pearson R	P-value	Partial pearson R	P-value
<b>NREM</b>				
Total slow and delta power, Anterior cortex	0.10	0.01	-0.04	0.28
Total slow and delta power, Thalamus	0.27	<0.001	-0.01	0.75
SO rate frontal, Anterior cortex	0.08	0.04	-0.01	0.72
SO rate frontal, Thalamus	0.20	<0.001	0.00	0.95
Slow spindles density frontal, Thalamus	0.19	<0.001	0.01	0.88
Slow spindles density frontal, Hippocampus	0.08	0.05	-0.02	0.67
Fast spindles density central, Thalamus	0.31	<0.001	0.11	0.01
Fast spindles density central, Hippocampus	0.17	<0.001	0.06	0.11
Total slow and delta power, MMSE	-0.01	0.86	-0.09	0.26
SO rate frontal, MMSE	-0.03	0.70	-0.09	0.27
Slow spindles density frontal, MMSE	0.17	0.03	0.10	0.20
Fast spindles density central, MMSE	0.20	0.01	0.10	0.20
Hippocampus, MMSE	0.20	0.01	0.12	0.15
Anterior cortex, MMSE	0.03	0.70	-0.04	0.60
Thalamus, MMSE	0.21	0.01	0.06	0.43
<b>REM</b>				
Percentage R, Isthmuscingulate	0.01	0.74	0.01	0.89
Percentage R, Amygdala	0.02	0.55	-0.02	0.71
Percentage R, Brainstem	0.02	0.58	0.02	0.55
Percentage R, MMSE	0.17	0.03	0.16	0.04
Isthmuscingulate, MMSE	0.06	0.48	0.08	0.33
Amygdala, MMSE	0.29	0.00	0.20	0.01
Brainstem, MMSE	0.03	0.69	0.03	0.73
<b>WAKE</b>				
Mean alpha during W, Thalamus	0.01	0.73	0.01	0.81
Mean alpha during W, Total ventricle volume	-0.04	0.36	-0.04	0.32
Mean alpha during W, MMSE	0.08	0.30	0.08	0.30
Total ventricle volume, MMSE	-0.24	<0.001	-0.15	0.07



directions and sizes of effects were largely consistent across the strata. However, due to a decrease in sample size, several feature pairs that showed significance with all participants did not reach significance within the individual strata. Notably, the strongest effect sizes differed among various disease and health groups for the investigated variable pairs. For example, the association of total delta power and the thalamic volume was stronger for patients with dementia compared to patients without disease and a Charlson Comorbidity index of less than 2 ( $r$  unadjusted = 0.34,  $p$  = 0.04;  $r$  unadjusted = 0.17,  $p$  = 0.10, respectively). Similar results were obtained for the fast spindle frequency and thalamic volume associations; and some relationships that were insignificant for all patients pooled showed significance in the hypothesized associations for specific groups, such as mean alpha during wake and MMSE scores for patients with dementia ( $r$  adjusted = 0.47,  $p$  = 0.03). This suggests that different diseases might alter function-structure-behavior relationships in distinct ways. The results of the analysis comparing variables from the a priori hypotheses

among patients with MCI, dementia, and control participants are presented in Figure 2.

### Part two: exploratory analyses.

We did a cluster analysis of the 776 selected features. These sleep features were then grouped into 24 distinct clusters. Among these clusters, nine were associated with N2 + N3 sleep stages, nine were associated with W + N1 sleep stages, five were related to REM sleep stages, and one cluster contained macro features. For the resulting cluster dendrograms, and a comprehensive list of sleep features included in each sleep cluster, please refer to [Supplementary Material](#).

To obtain  $p$ -values for the global associations, we employed the omnibus permutation procedure and obtained the following results: (1)  $p$ -values (all sleep features and brain structure volumes, cognition): best = 0.003, median = 0.0002. (2)  $p$ -values (all sleep features, cognition): best = 0.002, median = 0.001. (3)  $p$ -values (all brain structure volumes, cognition): best = 0.09, median = 0.001.

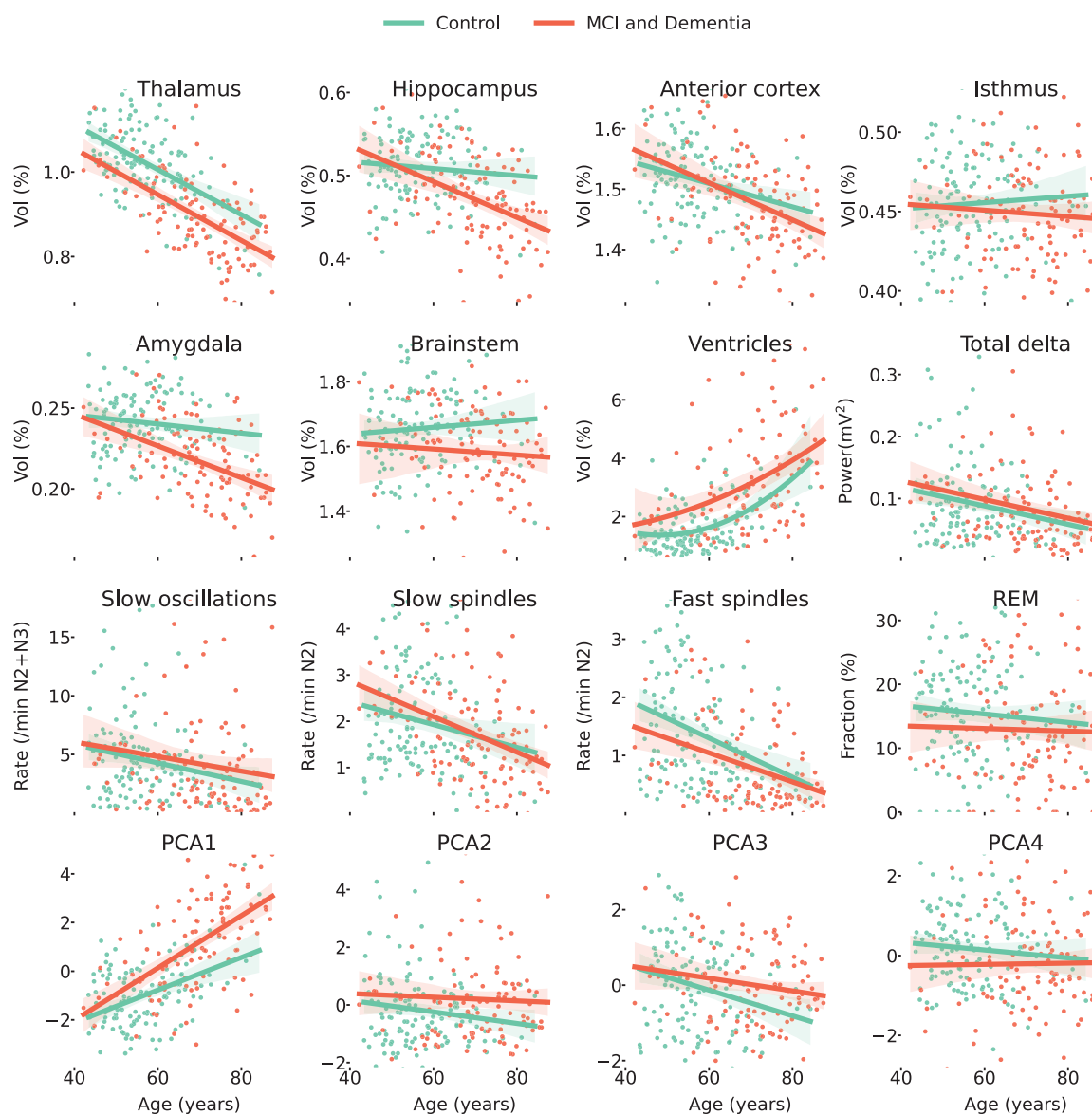


**Figure 2.** Differences of a priori hypotheses variables between dementia and controls.

		Cognition	Age	Thalamus	Hippocampus	Striatum	IPL	rACC	Ventricle	WM
N2N3	$\beta, \gamma$		** 0.08							
N2N3	S0, $\delta$		*** 0.11	*** 0.13		** 0.07	** 0.06	** 0.06	** 0.07	*** 0.08
N2N3	SP, $\sigma$	* 0.13	*** 0.20	*** 0.17	** 0.08	*** 0.17	* 0.06	*** 0.13	*** 0.19	*** 0.14
N2N3	S0, SP	* 0.09	*** 0.10	*** 0.10	*** 0.05	*** 0.08	** 0.04	*** 0.06	*** 0.08	*** 0.08
N2N3	$\delta/\theta$		** 0.09	* 0.06	* 0.07	* 0.06				
N2N3	$\delta/\alpha$ fast	* 0.14	** 0.09	** 0.10	* 0.07	*** 0.10		** 0.09	*** 0.12	*** 0.10
N2N3	S0, $\delta, \theta$		*** 0.20	*** 0.16		*** 0.15	** 0.08	** 0.08	*** 0.11	** 0.08
N2N3	$\beta$					* 0.06				
N2N3	$\alpha, \sigma, SP$		*** 0.24	*** 0.20	* 0.08	*** 0.20	* 0.07	*** 0.17	*** 0.18	*** 0.15
WN1	$\beta, \gamma$					* 0.08				
WN1	$\sigma$	** 0.20	* 0.07						* 0.07	
WN1	$\delta$ /fast	* 0.21		* 0.08		* 0.09			** 0.10	* 0.07
WN1	$\delta/\theta$		*** 0.14	** 0.09		* 0.07		* 0.06	* 0.07	
WN1	$\theta, \alpha$		** 0.10	** 0.09	* 0.08				*** 0.13	** 0.10
WN1	S0, $\delta$	* 0.16								
WN1	$\theta/\alpha$		*** 0.10	*** 0.15	*** 0.12	*** 0.14	*** 0.12	*** 0.09	*** 0.16	*** 0.14
WN1	STD		*** 0.12	*** 0.13	** 0.07	** 0.07	* 0.06	* 0.05	*** 0.13	* 0.06
WN1	S0/ $\delta$		* 0.07	** 0.08				* 0.06		
R	$\delta$ /fast	* 0.13								
R	$\delta, STD$		** 0.06	*** 0.07		** 0.05	* 0.05		*** 0.07	* 0.05
R	$\alpha, \sigma, \beta$	** 0.18	* 0.05							
R	$\delta, \theta/\alpha$	*** 0.23								
R	Timing			* 0.07		* 0.06				
Macro	Macro		*** 0.14	*** 0.11	* 0.06	*** 0.09	* 0.06	** 0.07	*** 0.11	*** 0.09

Figure 3. Results of all pairwise comparisons (Pearson correlation) between sleep feature clusters and cognition, age, and brain structure volumes.

Out of the 24 sleep clusters, nine were significantly associated with cognition and 17 with age, see Figure 3. Ten sleep clusters were significantly associated with the volume of at least one brain structure. The two brain structures with largest number of significantly associated sleep clusters were the thalamus and striatum with both 16 associated sleep clusters, followed by ventricles (14), white matter (12), anterior cortex (11), hippocampus (9), amygdala (9), and brainstem (5). Effect sizes were moderate. The sleep cluster with the largest absolute median correlation with cognition was “delta and theta/alpha power in REM sleep” ( $r = 0.23$  [0.12, 0.34],  $p < 0.001$ ), followed by “delta/fast power ratio in W+N1” ( $r = 0.21$  [0.14, 0.26],  $p < 0.05$ ) and “delta in W+N1” ( $r = 0.20$  [0.03, 0.32],  $p < 0.01$ ). The “N2+N3 alpha and sigma power,

and spindle activity” sleep cluster was the cluster most strongly associated with age ( $r = 0.24$  [0.01, 0.36],  $p < 0.001$ ) and specific brain structure volumes (thalamus:  $r = 0.20$  [0.03, 0.34],  $p < 0.001$ ; striatum:  $r = 0.20$  [0.02, 0.32],  $p < 0.001$ ).

The number of significantly correlated sleep features (out of all 776) per variable were: cognition 70, age 250, thalamus 240, striatum 182, hippocampus 54, amygdala 71, white matter 135, inferior parietal lobe 50, rostral anterior cingulate cortex 91, brainstem 22, and ventricles 208. The 35 sleep features with highest significance across any variable, excluding age, are shown in Figure 4. The top five features (theta power kurtosis in N2, fast sleep spindle density, EEG kurtosis in N2, alpha power kurtosis in N2, slow sleep spindle—SO coupling) are all stage N2 dependent

	Cognition	Age	Thalamus	Hippocampus	Striatum	IPL	rACC	Ventricle	WM
THETA BANDPOWER KURTOSIS F N2	***	-0.45	0.37	0.15	0.29	0.21	0.20	-0.29	0.25
FS DENS F	***	-0.38	0.34	0.18	0.28		0.20	-0.28	0.25
KURTOSIS C3-M2 N2	***	-0.38	0.32	0.15	0.21	0.16	0.16	-0.25	0.16
ALPHA BANDPOWER KURTOSIS F N2	***	-0.39	0.30		0.25		0.18	-0.21	0.22
SS COUPL OVERLAP F	***	-0.36	0.29		0.28	0.14	0.21	-0.24	0.23
THETA BANDPOWER KURTOSIS F W	***	-0.2	0.29	0.17	0.22	0.13	0.16	-0.24	0.19
SO DUR C	***	0.24	-0.29		-0.2	-0.19	-0.2	0.20	-0.22
HOURS SLEEP	***	-0.33	0.24	0.15	0.17		0.13	-0.25	0.15
THETA BANDPOWER KURTOSIS F N1	***	-0.2	0.26	0.19	0.19	0.16	0.16	-0.25	0.17
FS CHIRP C	***	-0.21	0.25	0.14	0.19	0.16	0.16	-0.23	0.14
FS SYMM F	***	0.21	-0.25		-0.17		-0.16	0.20	-0.14
THETA/ALPHA MEAN F W	*	-0.27	-0.21	-0.17	-0.18	-0.13		0.23	-0.19
FS CHIRP F	***	-0.24	0.23		0.14			-0.17	
SS CHIRP F	***	-0.23	0.22		0.15			-0.15	
SO DUR O	***	0.22	-0.22		-0.14			0.15	
SIGMA BANDPOWER KURTOSIS F W	***	-0.23	0.21		0.20	0.15		-0.15	0.13
PERC N1	***	0.18	-0.2		-0.13			0.12	
SS DENS F	***	-0.27	0.19		0.20		0.13	-0.2	0.18
FS COUPL MAG C	***	-0.16	0.20					-0.15	
SS ISA S C	***	-0.39							
ALPHA BANDPOWER MEAN F N2	***	-0.18	0.18		0.19		0.14	-0.15	0.14
MEAN GRADIENT C3-M2 R	***	-0.37							
FS COUPL ANGLE C	***	-0.27	0.19					-0.18	
THETA BANDPOWER KURTOSIS F N3	***	-0.26	0.19						
GAMMA BANDPOWER KURTOSIS F W	*	-0.14	0.13					***	
SIGMA BANDPOWER STD F W	***		0.18		0.14				0.15
THETA BANDPOWER MEAN F W	*	0.12	-0.14					0.18	
KURTOSIS F3-M2 N1	**	-0.16	0.18			0.14		-0.14	
SS CHIRP O	*	-0.14	0.19				0.16	-0.16	
BETA BANDPOWER KURTOSIS F N2	***	-0.2	0.18	0.16	0.19			-0.14	0.17
DELTA LINEAR B1	***	-0.18	0.19	0.14	0.18		0.15	-0.16	
SIGMA BANDPOWER KURTOSIS F N1	***	-0.2	0.14		0.18	0.13	0.14	-0.14	0.15
GAMMA BANDPOWER MEAN O R	***	-0.34							
KURTOSIS C4-M1 N3	***	-0.22	0.17						
FS COUPL ANGLE O	**	-0.16	0.18					**	*

**Figure 4.** Individual sleep feature associations were selected based on minimum Bonferroni-corrected p-value with cognition and the brain structure volumes.

and show similar association trends, i.e. negative associations with age and ventricle volume, and positive associations with volumes of thalamus, hippocampus, striatum, inferior parietal lobe, rostral anterior cingulate cortex and white matter. The duration of SOs, fast spindle symmetry, and theta–alpha power ratio during wake effectively show the opposite effect directions.

In the predictive analyses, we used R-squared ( $R^2$ ) as our primary evaluation metric, where a larger value indicates that more

of the variability is explained, and hence better model accuracy. Figure 5 shows the results for predicting cognition and age from MRI features, sleep features, and MRI and sleep EEG features combined. EEG predicted MMSE scores better than MRI ( $R^2 = 0.23$ , RMSE = 2.68, and  $R^2 = 0.16$ , RMSE = 2.79, respectively), while MRI predicted chronological age better than EEG ( $R^2 = 0.57$ , RMSE = 2.53, and  $R^2 = 0.48$ , RMSE = 2.66, respectively). In both tasks, combining EEG and MRI features leads to superior performance:  $R^2 = 0.4$ ,

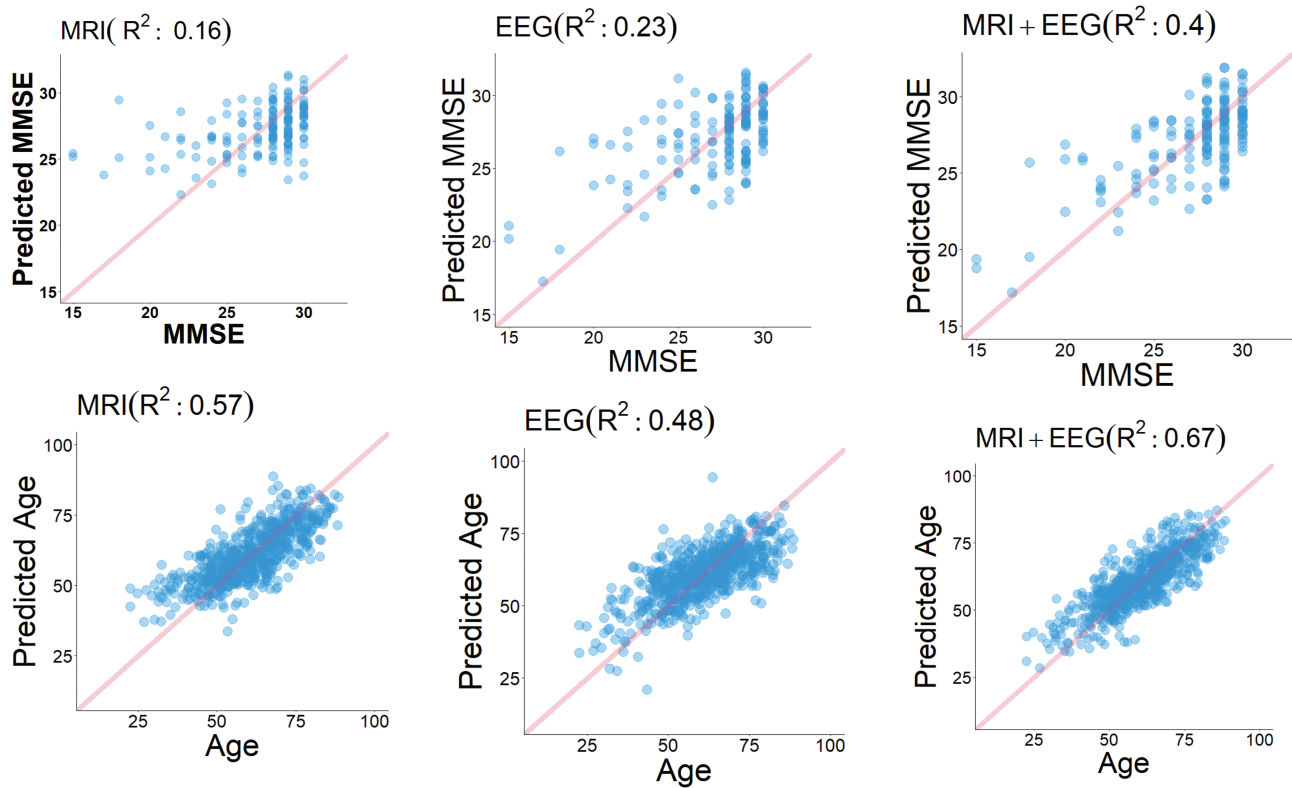


**Figure 5.** Leave-one-participant-out cross-validation (LOOCV) multivariate regression analysis.

RMSE = 2.36 for predicting MMSE, and  $R^2 = 0.67$ , RMSE = 2.39 for predicting age.

In [Figure 6A](#), the results for predicting MMSE and age are shown. Using all MRI + EEG features achieves the best performance, with a Pearson correlation between true and predicted values of 0.67 for MMSE and 0.82 for age. When using all EEG features, the Pearson correlations are 0.56 for MMSE and 0.69 for age, while using all MRI features yielded Pearson correlations of 0.43 for MMSE and 0.76 for age. Using a limited set of a priori hypothesized relevant EEG features resulted in a Pearson correlation of 0.15 for MMSE and 0.4 for age and using limited a priori features MRI features gave a Pearson correlation of 0.18 for MMSE and 0.7 for age. In [Figure 6B](#), the results for predicting brain structure and EEG variables are shown. In brain structure volume prediction tasks, the thalamus and total ventricle volumes were best predicted, with a Pearson correlation between true and predicted values of 0.61 for thalamus and 0.5 for total ventricle using all EEG features. When using a priori features EEG features, the Pearson correlations were 0.42 for thalamus and 0.31 for total ventricle volumes. In the EEG variable prediction task, fast spindle density and slow delta band power were able to be predicted best, with a Pearson correlation of 0.39 for fast spindle density and 0.28 for slow delta band power when using all MRI features, and 0.32 and 0.29, respectively when using a priori features only.

See [Supplementary Table S3](#) for a complete list of which input features were used in the prediction tasks, and the numerical values including confidence intervals, shown in [Figure 6](#).

## Discussion

We were able to derive a number of key findings from our analysis of heterogeneous clinical MRI and PSG data. In summary: (1) we verified a priori hypotheses. These include positive correlations between delta power and the volumes of specific frontal

lobe regions and the thalamus; positive correlations between sleep spindle density and the volumes of the thalamus and hippocampus; positive correlations between the percentage of REM sleep and cognitive test scores; and associations of brain structure volumes with dementia. It is noteworthy that some of these correlations weakened significantly after adjusting for age and sex., (2) Sensitivity analyses for different age and disease groups confirmed these results. Additionally, the effect sizes varied notably among the disease and health groups for the investigated variable pairs, suggesting distinct impacts of various diseases on function-structure-behavior relationships., (3) Structural predictions of REM sleep were not confirmed., (4) When analyzing functional and structural variables in people diagnosed with MCI or dementia versus controls, brain structure volume variables showed higher differentiation than sleep EEG features., (5) Combining MRI and sleep features best-predicted cognition., (6) Significant differences between MCI or dementia versus healthy participants were observed for thalamus, hippocampus, amygdala, brainstem, and total ventricle volumes., and (7) Both chronological age and cognitive MMSE scores were substantially predictable from function and structure variables.

Our study, despite its variable clinical nature, yielded reassuring results, confirming several known structure-function relationships related to sleep. Particularly, it reinforced the role of the thalamus and anterior cortex as significant sites of sleep slow-wave generation, and the thalamic reticular nucleus as the principal generator of sleep spindles. These spindles, representative of efficient cortical-subcortical connectivity, have been linked to memory-related abilities.

Several studies have also explored the associations between slow oscillatory activity in sleep EEG and brain structure variables. A summary of these studies, including those conducted exclusively in healthy participants as well as those focusing on

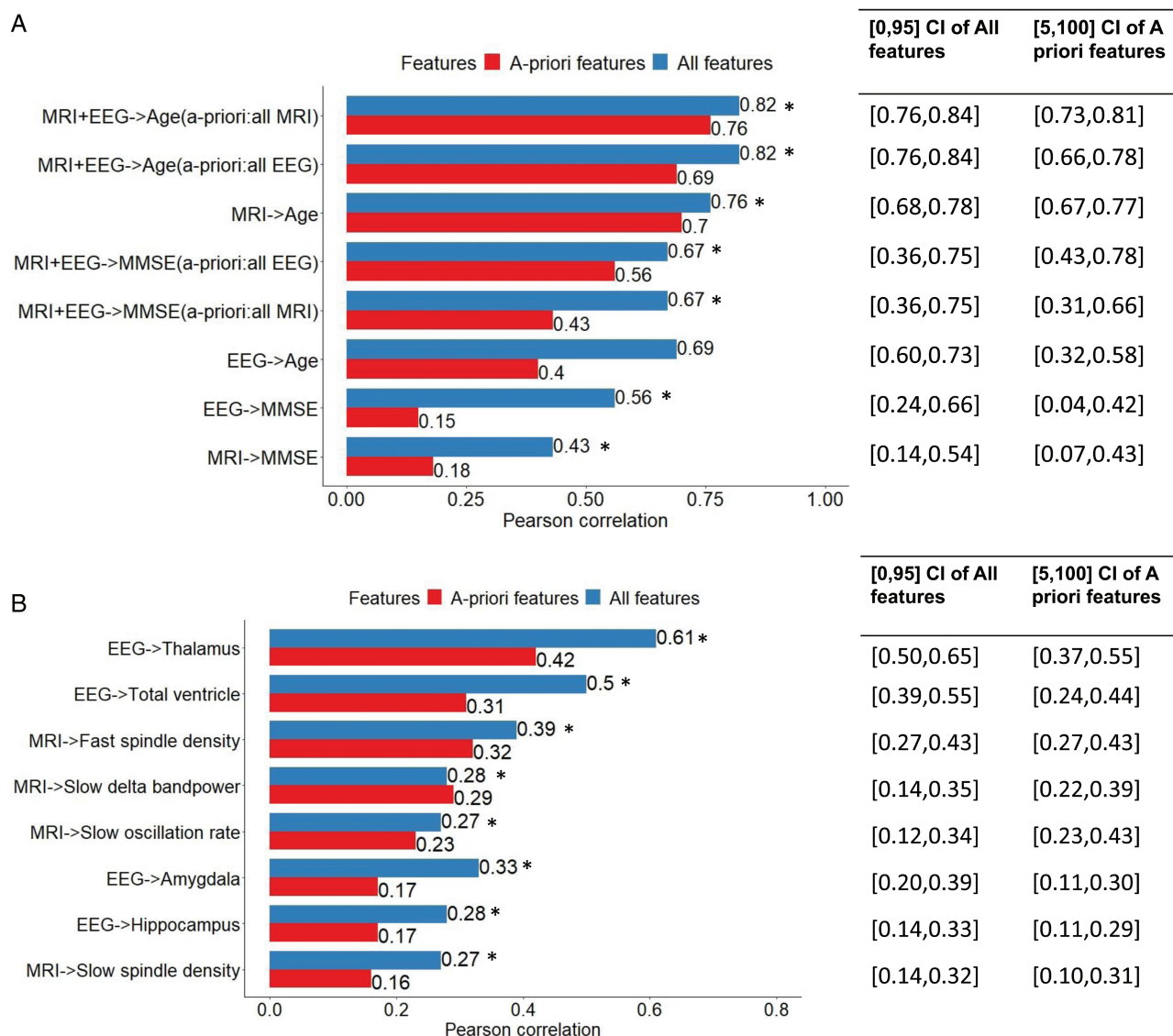


**Figure 6.** Leave-one-participant out cross-validation multivariate regression analysis.

specific diseases like schizophrenia and Alzheimer's Disease, can be found in Supplementary Table S3. Our analysis supports previous findings, but with an important exception. We found that the total delta power across a full night of sleep, as opposed to the slow wave rate, was associated with gray matter volume in the frontal lobe (sum of anterior cingulate cortex and medial orbitofrontal cortex) and the volume of the thalamus. This held true regardless of adjustments for age and sex. Essentially, our results highlight the total delta power, rather than slow wave rate, as a key variable in associations with certain brain structures. This distinction might be due to the fact that slow wave rate computations rely on identifying individual SOs using amplitude thresholds, a step not required when computing total delta power. In addition, we expand upon prior literature by assessing that sleep feature cluster consisting of SO and delta power features showed significant yet small-effect associations with the volumes of the thalamus, striatum, inferior parietal lobe, rostral anterior cingulate gyrus, ventricles, and white matter.

With regards to sleep spindles, building on Fogel et al.'s [39] findings of a positive association between sleep spindle density and hippocampal volume, we identified a significant association

of fast sleep spindle density with hippocampal volume prior to adjusting for age and sex ( $r=0.17$ ). However, this association became insignificant after the adjustments were made ( $r=0.06$ ). Confirming Buchmann et al.'s [86] results, our study further uncovered a small yet significant link between fast sleep spindle density and thalamic volume, both before adjustment ( $r=0.31$ ) and after ( $r=0.11$ ). In our exploratory analyses, the two NREM clusters containing sleep spindle features were among the clusters showing the largest and most consistent associations with volumes across different brain structures (thalamus, hippocampus, striatum, inferior parietal lobe, rostral anterior cingulate cortex, ventricles, and white matter). Individual sleep features driving those associations were fast spindle density, EEG signal kurtosis in N2 (indicating fluctuations), theta-alpha power kurtosis in N2, and SO-sleep spindle coupling.

Few studies have investigated relationships between features of REM sleep and brain structure. Reinhard et al. [87] found that the thickness of the left caudal anterior cingulate cortex was positively associated with the 24-32 Hz EEG beta power band during REM sleep. Baril et al. [88] found no associations between REM sleep and MRI markers. While none of our a priori REM

sleep—brain structure (isthmus cingulate, amygdala, brainstem) hypotheses showed significance, both percentage of REM sleep and the volume of the amygdala were associated with cognition ( $r = 0.16$  and  $r = 0.20$ , respectively). In the exploratory analysis, two REM clusters were associated with brain structures: a cluster containing delta power and EEG fluctuation features was associated with the volumes of the thalamus, striatum, ventricles, white matter and inferior parietal lobe, and a cluster containing features about REM timing was associated with thalamic and striatal volumes. Neuroimaging correlates of REM sleep may be limited by the spatial resolution of current scanners for the subcortex/brainstem, which may be overcome by high field (e.g. 7 Tesla) imaging in combination with concordant updates to Freesurfer and SynthSeg software that use atlases generated from the higher-resolution images.

Cognitive MMSE scores and chronological age (as a measure of brain aging) were both predictable from function and structure. When predicting MMSE ( $N = 160$ ), using EEG variables as predictors resulted in better prediction performance than using MRI variables ( $r$ -squared 0.23 vs. 0.16, respectively). When predicting age, MRI features resulted in better predictive performance compared to EEG ( $R$ -squared 0.57 vs. 0.48). In both tasks, combining MRI and EEG variables lead to superior performances (MMSE  $R$ -squared 0.4, age  $R$ -squared 0.67). The prediction performance decreased mild to moderately when we used only features that were part of our a priori hypotheses—thus, using specific variables ranging from spectral features, complexity features to spindle/slow-oscillation features improved predictive performance compared to using only well-known and established sleep/structure variables. This phenomenon was true as well when we predicted specific structure variables from all versus limited EEG features and specific EEG features from all vs. limited MRI features.

We revealed intricate associations between sleep EEG function, brain structure as determined by MRI, and cognition assessed by MMSE scores. We observed moderate effect sizes between these factors before controlling for age and sex, which were significantly reduced after these demographic variables were taken into account. This highlights that while age and sex can indeed explain a considerable portion of the structure-function-cognition relationships, there exist meaningful residual associations that persist even after controlling for these variables. Intriguingly, each link within this triangle of sleep function, brain structure, and cognition seems to harbor unique information that isn't wholly encapsulated by any other pair, revealing an intriguing pattern of pairwise non-overlapping insights. This was evidenced in both our a priori hypothesis testing, for instance, where REM sleep and the amygdala each demonstrated significant correlations with MMSE performance yet showed no significant interrelation, and in our predictive analyses. Here, we found that while either EEG or MRI data alone could reasonably predict cognitive performance, a combined approach resulted in improved accuracy. This underscores the importance of an integrated, holistic view of the relationship between sleep, brain structure, and cognition.

How may this type of information be clinically useful and impact patient care? The polysomnogram provides information about brain, cardiac, respiratory, and lung health at a minimum. Beyond the usual “numbers” used clinically (such as the apnea-hypopnea index and hypoxic impacts), even using the standard sleep stages provides information about brain health (visually poor spindling or age-disproportionate excessive N3 age), lung health (disproportionate desaturation for mild respiratory events)

or cardiac systolic/diastolic function (long-cycle periodic breathing). There are numerous examples of “useful and meaningful incidental findings” in clinical testing, including silent brain tumors-MRI, old myocardial infarctions-ECG, adrenal tumor-MRI, lung cancer (chest computerized tomography), sleep apnea risk estimation (cephalometry), and numerous blood biomarkers, as examples. The data from polysomnography is largely discarded, and combined with clinical brain MRI, could in an automated fashion provide “incidental” risk information for brain health. Polysomnography is increasingly restricted to older sicker patients (home sleep testing siphons off the more classic apnea), the exact population where brain health concerns are increasing. Extracting the maximum useful information from clinical testing is a reasonable strategy if not burdensome. The combination of MRI with sleep data may also be a way to assess improvements in brain health with disease-modifying therapies, using machine learning approaches. This includes not only possibly risk stratifying for early dementia but also brain health in conditions such as depression, post-traumatic stress disorder and schizophrenia. The increasing availability of ambulatory EEG raises the possibility of automated tracking of brain health through the type of analysis we present, though it needs to be validated using home recording devices.

Our study has important limitations. The study design was cross-sectional; therefore, we could not assess longitudinal changes within participants. Furthermore, we used single sleep, MRI, and cognition measures per participant which were as far as 5 years apart. Associations could be estimated more robustly with multiple visits and the measures if collected closer in time. The diversity of participants' health conditions, which on the one hand is a strength of our study, comes with disadvantages as well, as the confounding effects of the different diagnoses may not be fully controlled. These comorbid conditions can influence sleep patterns and brain structure independently of each other. Also, although MRI sequences varied widely across participants, we did not explore issues such as how the choice of acquisition sequences in the scan was related to the clinical indication for the scan, perhaps leading to biases such as more accurate brain volume predictions for older or sicker patients. In EEG data processing, we adopted amplitude-based artifact rejection criteria for its simplicity and consistent application across datasets and participants, though the results depend somewhat on the chosen threshold. Furthermore, there is likely a selection bias as the participants were from a hospital setting, limiting generalizability of the findings to the wider population. Neuropsychological evaluation data were only available for a subset of the participants and assessed via the MMSE score only. Although this study was able to predict chronological age and cognitive MMSE scores from functional and structural variables, the predictive performance varied, and the robustness of these models may need further evaluation. This is particularly true when considering the small effect sizes in some of the associations.

In summary, we confirmed previously hypothesized associations between sleep patterns and brain structures using data extracted from routine clinical sleep studies and MR images. The finding that data-driven selection of EEG and MRI features perform substantially better than hypothesis-driven features for predicting cognitive status and age suggests that multivariable analytics may have a role in practice. The study demonstrates the potential for an expanded use of clinical EEG and structural MRI data for future studies and possibly automated analysis to aid clinical practice.

## Supplementary Material

Supplementary material is available at *SLEEP* online.

## Funding

This work was supported by the NIH (R01NS102190, R01NS102574, R01NS107291, RF1AG064312, RF1NS120947, R01AG073410, R01HL161253, R01NS126282, R01AG073598, 1RF1MH123195, 1R01AG070988, 1R01EB031114, 1UM1MH130981, and P41EB015902), and NSF (2014431), ERC Starting Grant (677697), ARUK grant (IRG2019A-003).

## Disclosure Statement

The authors report no competing interests.

## Author Contribution

Ruoqi Wei, MD, PhD: Together with WG principal contributor to research. Identifying patients included in the study, carrying out preprocessing for MRI and cognitive data, develop code for analyses and visualization for [Figures 1](#), [5](#), and [6](#), original draft preparation and reviewing. Wolfgang Ganglberger, MS: Together with RW principal contributor to research, carrying out computation of sleep features, develop code for analyses and visualizations for [Figures 2](#), [3](#), [4](#), and drafting and reviewing the manuscript. Haoqi Sun, PhD, provided substantial advisory input and feedback during the analysis process, review of the manuscript. Peter Hadar, MD, Randy Gollub, MD, PhD, and Steve Pieper, PhD, played key roles in quality assurance for the MRI data, ensuring its accuracy and reliability for subsequent analysis. Benjamin Billot, PhD, Rhoda Au, PhD, Juan Eugenio Iglesias, Ph.D., Sydney S. Cash, MD, PhD, Soriul Kim, PhD, and Chol Shin, MD, PhD, contributed significantly through providing feedback on the analysis and performing a review of the manuscript. M. Brandon Westover, MD, PhD, and Robert Joseph Thomas, MD, served as the supervisors for the entire project, and reviewed the manuscript in its entirety.

## Data Availability

The data that support the findings of this study are available from the corresponding author, upon reasonable request.

## References

- Prinz PN, Vitaliano PP, Vitiello MV, et al. Sleep, EEG and mental function changes in senile dementia of the Alzheimer's type. *Neurobiol Aging*. 1982;**3**(4):361–370. doi: [10.1016/0197-4580\(82\)90024-0](#)
- Pase MP, Himali JJ, Grima NA, et al. Sleep architecture and the risk of incident dementia in the community. *Neurology*. 2017;**89**(12):1244–1250. doi: [10.1212/WNL.0000000000004373](#)
- Varga AW, Kishi A, Mantua J, et al. Apnea-induced rapid eye movement sleep disruption impairs human spatial navigational memory. *J Neurosci*. 2014;**34**(44):14571–14577. doi: [10.1523/JNEUROSCI.3220-14.2014](#)
- Bjorness TE, Riley BT, Tysor MK, Poe GR. REM restriction persistently alters strategy used to solve a spatial task. *Learn Mem*. 2005;**12**(3):352–359. doi: [10.1101/lm.84805](#)
- Smith C, Rose GM. Evidence for a paradoxical sleep window for place learning in the Morris water maze. *Physiol Behav*. 1996;**59**(1):93–97. doi: [10.1016/0031-9384\(95\)02054-3](#)
- Mander BA, Winer JR, Jagust WJ, Walker MP. Sleep: A novel mechanistic pathway, biomarker, and treatment target in the pathology of alzheimer's disease? *Trends Neurosci*. 2016;**39**(8):552–566. doi: [10.1016/j.tins.2016.05.002](#)
- Lafortune M, Gagnon JF, Martin N, et al. Sleep spindles and rapid eye movement sleep as predictors of next morning cognitive performance in healthy middle-aged and older participants. *J Sleep Res*. 2014;**23**(2):159–167. doi: [10.1111/jsr.12108](#)
- Helfrich RF, Mander BA, Jagust WJ, Knight RT, Walker MP. Old brains come uncoupled in sleep: Slow wave-spindle synchrony, brain atrophy, and forgetting. *Neuron*. 2018;**97**(1):221–230.e4. doi: [10.1016/j.neuron.2017.11.020](#)
- Muehlroth BE, Sander MC, Fandakova Y, et al. Precise slow oscillation-spindle coupling promotes memory consolidation in younger and older adults. *Sci Rep*. 2019;**9**(1):1940–1940. doi: [10.1038/s41598-018-36557-z](#)
- Steriade M, Deschênes M. Inhibitory processes in the thalamus. *J Mind Behav*. 1987;**59**:559–571.
- Luethi A. Sleep spindles: Where they come from, what they do. *Neurosci*. 2014;**20**(3):243–256. doi: [10.1177/1073858413500854](#)
- Niethard N, Ngo H-VV, Ehrlich I, Born J. Cortical circuit activity underlying sleep slow oscillations and spindles. *Proc Natl Acad Sci USA*. 2018;**115**(39):E9220–E9229. doi: [10.1073/pnas.1805517115](#)
- Helfrich RF, Lendner JD, Mander BA, et al. Bidirectional prefrontal-hippocampal dynamics organize information transfer during sleep in humans. *Nat Commun*. 2019;**10**(1):3572–3516. doi: [10.1038/s41467-019-11444-x](#)
- Astori S, Wimmer RD, Lüthi A. Manipulating sleep spindles—expanding views on sleep, memory, and disease. *Trends Neurosci*. 2013;**36**(12):738–748. doi: [10.1016/j.tins.2013.10.001](#)
- Weng Y-Y, Lei X, Yu J. Sleep spindle abnormalities related to Alzheimer's disease: A systematic mini-review. *Sleep Med*. 2020;**75**:37–44. doi:[10.1016/j.sleep.2020.07.044](#)
- Gorgoni M, Lauri G, Truglia I, et al. Parietal fast sleep spindle density decrease in Alzheimer's disease and amnesic mild cognitive impairment. *Neural Plast*. 2016;**2016**:8376108–8376108. doi:[10.1155/2016/8376108](#)
- Latreille V, Carrier J, Lafortune M, et al. Sleep spindles in Parkinson's disease may predict the development of dementia. *Neurobiol Aging*. 2015;**36**(2):1083–1090. doi: [10.1016/j.neurobiolaging.2014.09.009](#)
- Rauchs G, Schabus M, Parapatics S, et al. Is there a link between sleep changes and memory in Alzheimer's disease? *Neuroreport*. 2008;**19**(11):1159–1162. doi: [10.1097/WNR.0b013e32830867c4](#)
- Ohayon MM, Vecchierini MF. Normative sleep data, cognitive function and daily living activities in older adults in the community. *Sleep*. 2005;**28**(8):981–989. doi: [10.1093/sleep/28.8.981](#)
- Keage HAD, Banks S, Yang KL, Morgan K, Brayne C, Matthews FE. What sleep characteristics predict cognitive decline in the elderly? *Sleep Med*. 2012;**13**(7):886–892. doi: [10.1016/j.sleep.2012.02.003](#)
- Song Y, Blackwell T, Yaffe K, Ancoli-Israel S, Redline S, Stone KL; Osteoporotic Fractures in Men (MrOS) Study Group. Relationships between sleep stages and changes in cognitive function in older men: The MrOS sleep study. *Sleep*. 2015;**38**(3):411–421. doi: [10.5665/sleep.4500](#)
- Cavuoto MG, Ong B, Pike KE, Nicholas CL, Bei B, Kinsella GJ. Objective but not subjective sleep predicts memory in

- community-dwelling older adults. *J Sleep Res.* 2016;**25**(4):475–485. doi: [10.1111/jsr.12391](https://doi.org/10.1111/jsr.12391)
23. Blackwell T, Yaffe K, Ancoli-Israel S, et al.; Osteoporotic Fractures in Men Study Group. Associations between sleep architecture and sleep-disordered breathing and cognition in older community-dwelling men: The osteoporotic fractures in men sleep study. *J Am Geriatr Soc.* 2011;**59**(12):2217–2225. doi: [10.1111/j.1532-5415.2011.03731.x](https://doi.org/10.1111/j.1532-5415.2011.03731.x)
  24. Spira AP, Stone KL, Redline S, et al. Actigraphic sleep duration and fragmentation in older women: Associations with performance across cognitive domains. *Sleep.* 2017;**40**(8):zsx073–zsx073. doi:[10.1093/sleep/zsx073](https://doi.org/10.1093/sleep/zsx073)
  25. Devore EE, Grodstein F, Duffy JF, Stampfer MJ, Czeisler CA, Schernhammer ES. Sleep duration in midlife and later life in relation to cognition. *J Am Geriatr Soc.* 2014;**62**(6):1073–1081. doi: [10.1111/jgs.12790](https://doi.org/10.1111/jgs.12790)
  26. Ramos AR, Tarraf W, Daviglius M, et al. Sleep duration and neurocognitive function in the hispanic community health study/ study of latinos. *Sleep.* 2016;**39**(10):1843–1851. doi: [10.5665/sleep.6166](https://doi.org/10.5665/sleep.6166)
  27. Purcell SM, Manoach DS, Demanuele C, et al. Characterizing sleep spindles in 11,630 individuals from the National Sleep Research Resource. *Nat Commun.* 2017;**8**(1):15930–15930. doi: [10.1038/ncomms15930](https://doi.org/10.1038/ncomms15930)
  28. Espiritu JRD. Aging-related sleep changes. *Clin Geriatr Med.* 2008;**24**(1):1–14, v. doi: [10.1016/j.cger.2007.08.007](https://doi.org/10.1016/j.cger.2007.08.007)
  29. Feige B, Al-Shajlawi A, Nissen C, et al. Does REM sleep contribute to subjective wake time in primary insomnia? A comparison of polysomnographic and subjective sleep in 100 patients. *J Sleep Res.* 2008;**17**(2):180–190. doi: [10.1111/j.1365-2869.2008.00651.x](https://doi.org/10.1111/j.1365-2869.2008.00651.x)
  30. Mander BA, Winer JR, Walker MP. Sleep and human aging. *Neuron.* 2017;**94**(1):19–36. doi: [10.1016/j.neuron.2017.02.004](https://doi.org/10.1016/j.neuron.2017.02.004)
  31. Scullin MK. Do older adults need sleep? a review of neuroimaging, sleep, and aging studies. *Curr Sleep Med Rep.* 2017;**3**(3):204–214. doi: [10.1007/s40675-017-0086-z](https://doi.org/10.1007/s40675-017-0086-z)
  32. Carrier J, Land S, Buysse DJ, Kupfer DJ, Monk TH. The effects of age and gender on sleep EEG power spectral density in the middle years of life (ages 20-60 years old). *Psychophysiology.* 2001;**38**(2):232–242. doi: [10.1017/S0048577201991838](https://doi.org/10.1017/S0048577201991838)
  33. Larsen LH, Moe KE, Vitiello MV, Prinz PN. Age trends in the sleep EEG of healthy older men and women. *J Sleep Res.* 1995;**4**(3):160–172. doi: [10.1111/j.1365-2869.1995.tb00165.x](https://doi.org/10.1111/j.1365-2869.1995.tb00165.x)
  34. Dube J, Lafortune M, Bedetti C, et al. Cortical thinning explains changes in sleep slow waves during adulthood. *J Neurosci.* 2015;**35**(20):7795–7807. doi: [10.1523/JNEUROSCI.3956-14.2015](https://doi.org/10.1523/JNEUROSCI.3956-14.2015)
  35. Breen DP, Vuono R, Nawarathna U, et al. Sleep and circadian rhythm regulation in early Parkinson disease. *JAMA Neurol.* 2014;**71**(5):589–595. doi: [10.1001/jamaneurol.2014.65](https://doi.org/10.1001/jamaneurol.2014.65)
  36. Comella C. Sleep disturbances and excessive daytime sleepiness in Parkinson disease: An overview. *Parkinson's Dis Related Disord.* 2006;**70**:349–355.
  37. Frauscher B, Bernasconi N, Caldarour B, et al. Interictal hippocampal spiking influences the occurrence of hippocampal sleep spindles. *Sleep.* 2015;**38**(12):1927–1933. doi: [10.5665/sleep.5242](https://doi.org/10.5665/sleep.5242)
  38. Mander BA, Rao V, Lu B, et al. Impaired prefrontal sleep spindle regulation of hippocampal-dependent learning in older adults. *Cereb Cortex.* 2014;**24**(12):3301–3309. doi: [10.1093/cercor/bht188](https://doi.org/10.1093/cercor/bht188)
  39. Fogel S, Vien C, Karni A, Benali H, Carrier J, Doyon J. Sleep spindles: A physiological marker of age-related changes in gray matter in brain regions supporting motor skill memory consolidation. *Neurobiol Aging.* 2017;**49**:154–164. doi: [10.1016/j.neurobiolaging.2016.10.009](https://doi.org/10.1016/j.neurobiolaging.2016.10.009)
  40. Martin N, Lafortune M, Godbout J, et al. Topography of age-related changes in sleep spindles. *Neurobiol Aging.* 2013;**34**(2):468–476. doi: [10.1016/j.neurobiolaging.2012.05.020](https://doi.org/10.1016/j.neurobiolaging.2012.05.020)
  41. Diering GH, Nirujogi RS, Roth RH, Worley PF, Pandey A, Hugarir RL. Homer1a drives homeostatic scaling-down of excitatory synapses during sleep. *Science.* 2017;**355**(6324):511–515. doi: [10.1126/science.aai8355](https://doi.org/10.1126/science.aai8355)
  42. Wilson MA, McNaughton BL. Reactivation of hippocampal ensemble memories during sleep. *Science.* 1994;**265**(5172):676–679. doi: [10.1126/science.8036517](https://doi.org/10.1126/science.8036517)
  43. Stickgold R, Walker MP. Sleep-dependent memory consolidation and reconsolidation. *Sleep Med.* 2007;**8**(4):331–343. doi: [10.1016/j.sleep.2007.03.011](https://doi.org/10.1016/j.sleep.2007.03.011)
  44. De Vivo L, Bellesi M, Marshall W, et al. Ultrastructural evidence for synaptic scaling across the wake/sleep cycle. *Science.* 2017;**355**(6324):507–510. doi: [10.1126/science.aah5982](https://doi.org/10.1126/science.aah5982)
  45. Djonlagic I, Mariani S, Fitzpatrick AL, et al. Macro and micro sleep architecture and cognitive performance in older adults. *Nat Hum Behav.* 2021;**5**(1):123–145. doi: [10.1038/s41562-020-00964-y](https://doi.org/10.1038/s41562-020-00964-y)
  46. Yaffe K, Laffan AM, Harrison SL, et al. Sleep-disordered breathing, hypoxia, and risk of mild cognitive impairment and dementia in older women. *JAMA: the journal of the American Medical Association.* 2011;**306**(6):613–619. doi: [10.1001/jama.2011.1115](https://doi.org/10.1001/jama.2011.1115)
  47. Winer JR, Mander BA. Waking up to the importance of sleep in the pathogenesis of alzheimer disease. *JAMA Neurol.* 2018;**75**(6):654–656. doi: [10.1001/jamaneurol.2018.0005](https://doi.org/10.1001/jamaneurol.2018.0005)
  48. Haydon PG. Astrocytes and the modulation of sleep. *Curr Opin Neurobiol.* 2017;**44**:28–33. doi: [10.1016/j.conb.2017.02.008](https://doi.org/10.1016/j.conb.2017.02.008)
  49. Ju YS, Ooms SJ, Sutphen C, et al. Slow wave sleep disruption increases cerebrospinal fluid amyloid-beta levels. *Brain.* 2017;**140**(8):2104–2111. doi: [10.1093/brain/awx148](https://doi.org/10.1093/brain/awx148)
  50. Sun H, Ye E, Paixao L, et al. The sleep and wake electroencephalogram over the lifespan. *Neurobiol Aging.* 2023;**124**:60–70. doi: [10.1016/j.neurobiolaging.2023.01.006](https://doi.org/10.1016/j.neurobiolaging.2023.01.006)
  51. Killgore WD. Effects of sleep deprivation on cognition. *Prog Brain Res.* 2010;**185**:105–129. doi: [10.1016/B978-0-444-53702-7.00007-5](https://doi.org/10.1016/B978-0-444-53702-7.00007-5)
  52. Krause AJ, Simon EB, Mander BA, et al. The sleep-deprived human brain. *Nat Rev Neurosci.* 2017;**18**(7):404–418. doi: [10.1038/nrn.2017.55](https://doi.org/10.1038/nrn.2017.55)
  53. Hobson JA, Pace-Schott EF. The cognitive neuroscience of sleep: Neuronal systems, consciousness and learning. *Nat Rev Neurosci.* 2002;**3**(9):679–693. doi: [10.1038/nrn915](https://doi.org/10.1038/nrn915)
  54. French IT, Muthusamy KA. A review of sleep and its disorders in patients with parkinson's disease in relation to various brain structures. *Front Aging Neurosci.* 2016;**8**:114. doi: [10.3389/fnagi.2016.00114](https://doi.org/10.3389/fnagi.2016.00114)
  55. Li Y, Sahakian BJ, Kang J, et al. The brain structure and genetic mechanisms underlying the nonlinear association between sleep duration, cognition and mental health. *Nature Aging.* 2022;**2**(5):425–437. doi: [10.1038/s43587-022-00210-2](https://doi.org/10.1038/s43587-022-00210-2)
  56. Canessa N, Castronovo V, Cappa SF, et al. Obstructive sleep apnea: brain structural changes and neurocognitive function before and after treatment. *Am J Respir Crit Care Med.* 2011;**183**(10):1419–1426. doi: [10.1164/rccm.201005-0693OC](https://doi.org/10.1164/rccm.201005-0693OC)
  57. Westerberg CE, Lundgren EM, Florczak SM, et al. Sleep influences the severity of memory disruption in amnesic mild cognitive impairment: Results from sleep self-assessment and continuous activity monitoring. *Alzheimer Dis Assoc Disord.* 2010;**24**(4):325–333. doi: [10.1097/WAD.0b013e3181e30846](https://doi.org/10.1097/WAD.0b013e3181e30846)
  58. Wardlaw JM, Benveniste H, Nedergaard M, et al.; colleagues from the Fondation Leducq Transatlantic Network of Excellence on the Role of the Perivascular Space in Cerebral Small Vessel



- Disease. Perivascular spaces in the brain: Anatomy, physiology and pathology. *Nat Rev Neurol*. 2020;**16**(3):137–153. doi: [10.1038/s41582-020-0312-z](https://doi.org/10.1038/s41582-020-0312-z)
59. Parrino L, Vaudano AE. The resilient brain and the guardians of sleep: New perspectives on old assumptions. *Sleep Med Rev*. 2018;**39**:98–107. doi: [10.1016/j.smrv.2017.08.003](https://doi.org/10.1016/j.smrv.2017.08.003)
  60. Sun H, Paixao L, Oliva JT, et al. Brain age from the electroencephalogram of sleep. *Neurobiol Aging*. 2019;**74**:112–120. doi: [10.1016/j.neurobiolaging.2018.10.016](https://doi.org/10.1016/j.neurobiolaging.2018.10.016)
  61. Paixao L, Sikka P, Sun H, et al. Excess brain age in the sleep electroencephalogram predicts reduced life expectancy. *Neurobiol Aging*. 2020;**88**:150–155. doi: [10.1016/j.neurobiolaging.2019.12.015](https://doi.org/10.1016/j.neurobiolaging.2019.12.015)
  62. Pham DL, Xu C, Prince JL. A survey of current methods in medical image segmentation. *Annu Rev Biomed Eng*. 2000;**2**(3):315–337. doi: [10.1146/annurev.bioeng.2.1.315](https://doi.org/10.1146/annurev.bioeng.2.1.315)
  63. Billot B, Greve DN, Puonti O, et al.; ADNI. SynthSeg: Segmentation of brain MRI scans of any contrast and resolution without retraining. *Med Image Anal*. 2023;**86**:102789–102789. doi: [10.1016/j.media.2023.102789](https://doi.org/10.1016/j.media.2023.102789)
  64. Billot B, Magdamo C, Cheng Y, Arnold SE, Das S, Iglesias JE. Robust machine learning segmentation for large-scale analysis of heterogeneous clinical brain MRI datasets. *Proc Natl Acad Sci USA*. 2023;**120**(9):e2216399120. doi: [10.1073/pnas.2216399120](https://doi.org/10.1073/pnas.2216399120)
  65. Massimini M, Huber R, Ferrarelli F, Hill S, Tononi G. The sleep slow oscillation as a traveling wave. *J Neurosci*. 2004;**24**(31):6862–6870. doi: [10.1523/JNEUROSCI.1318-04.2004](https://doi.org/10.1523/JNEUROSCI.1318-04.2004)
  66. Landolt H-P, Dijk D-J, Achermann P, Borbély AA. Effect of age on the sleep EEG: Slow-wave activity and spindle frequency activity in young and middle-aged men. *Brain Res*. 1996;**738**(2):205–212. doi: [10.1016/s0006-8993\(96\)00770-6](https://doi.org/10.1016/s0006-8993(96)00770-6)
  67. Varga AW, Ducca EL, Kishi A, et al. Effects of aging on slow wave sleep dynamics and human spatial navigational memory consolidation. *Neurobiol Aging*. 2015;**42**:142–149. doi: [10.1016/j.neurobiolaging.2016.03.008](https://doi.org/10.1016/j.neurobiolaging.2016.03.008)
  68. Colom LV, Garrido-Sanabria E. Modulation of normal and altered hippocampal excitability states by septal networks. *J Neurosci Res*. 2007;**85**(13):2839–2843. doi: [10.1002/jnr.21276](https://doi.org/10.1002/jnr.21276)
  69. Dahl MJ, Mather M, Werkle-Bergner M. Noradrenergic modulation of rhythmic neural activity shapes selective attention. *Trends Cogn Sci*. 2022;**26**(1):38–52. doi: [10.1016/j.tics.2021.10.009](https://doi.org/10.1016/j.tics.2021.10.009)
  70. Li X, Yang X, Sun Z. Alpha rhythm slowing in a modified thalamo-cortico-thalamic model related with Alzheimer's disease. *PLoS One*. 2020;**15**(3):e0229950. doi: [10.1371/journal.pone.0229950](https://doi.org/10.1371/journal.pone.0229950)
  71. Waser M, Benke T, Dal-Bianco P, et al. Neuroimaging markers of global cognition in early Alzheimer's disease: A magnetic resonance imaging–electroencephalography study. *Brain Behav*. 2019;**9**(1):e01197.
  72. Hulbert S, Adeli H. EEG/MEG-and imaging-based diagnosis of Alzheimer's disease. *Rev Neurosci*. 2013;**24**(6):563–576. doi: [10.1515/revneuro-2013-0042](https://doi.org/10.1515/revneuro-2013-0042)
  73. JesusBjr, Cassani R, McGeown WJ, Cecchi M, Fadem K, Falk TH. Multimodal prediction of Alzheimer's disease severity level based on resting-state EEG and structural MRI. *Front Hum Neurosci*. 2021;**15**:700627.
  74. Fischl B. FreeSurfer. *Neuroimage*. 2012;**62**(2):774–781. doi: [10.1016/j.neuroimage.2012.01.021](https://doi.org/10.1016/j.neuroimage.2012.01.021)
  75. Voevodskaya O, Simmons A, Nordenskjöld R, et al.; Alzheimer's Disease Neuroimaging Initiative. The effects of intracranial volume adjustment approaches on multiple regional MRI volumes in healthy aging and Alzheimer's disease. *Front Aging Neurosci*. 2014;**6**:264. doi: [10.3389/fnagi.2014.00264](https://doi.org/10.3389/fnagi.2014.00264)
  76. Nordenskjöld R, Malmberg F, Larsson E-M, et al. Intracranial volume normalization methods: Considerations when investigating gender differences in regional brain volume. *Psychiatry Res*. 2015;**231**(3):227–235. doi: [10.1016/j.psychresns.2014.11.011](https://doi.org/10.1016/j.psychresns.2014.11.011)
  77. Berry RB, Brooks R, Gamaldo CE, Harding SM, Marcus C, Vaughn BV. The AASM manual for the scoring of sleep and associated events. *Am Acad Sleep Med*. 2012;**176**:2012.
  78. Morrell MJ, Finn L, Kim H, Peppard PE, Safwan Badr M, Young T. Sleep fragmentation, awake blood pressure, and sleep-disordered breathing in a population-based study. *Am J Respir Crit Care Med*. 2000;**162**(6):2091–2096.
  79. Sun H, Jia J, Goparaju B, et al. Large-scale automated sleep staging. *Sleep*. 2017;**40**(10). doi: [10.1093/sleep/zsx139](https://doi.org/10.1093/sleep/zsx139)
  80. Purcell S, Manoach D, Demanuele C, et al. Characterizing sleep spindles in 11,630 individuals from the national sleep research resource. *Nat Commun*. 2017;**8**(1):15930.
  81. WardHJr. Hierarchical grouping to optimize an objective function. *J Am Stat Assoc*. 1963;**58**(301):236–244. doi: [10.1080/01621459.1963.10500845](https://doi.org/10.1080/01621459.1963.10500845)
  82. Ye E, Sun H, Leone MJ, et al. Association of sleep electroencephalography-based brain age index with dementia. *JAMA Netw Open*. 2020;**3**(9):e2017357–e2017357. doi: [10.1001/jamanetworkopen.2020.17357](https://doi.org/10.1001/jamanetworkopen.2020.17357)
  83. van Steenoven I, Aarsland D, Hurtig H, et al. Conversion between mini-mental state examination, montreal cognitive assessment, and dementia rating scale-2 scores in Parkinson's disease. *Mov Disord*. 2014;**29**(14):1809–1815. doi: [10.1002/mds.26062](https://doi.org/10.1002/mds.26062)
  84. Vehtari A, Gelman A, Gabry J. Practical Bayesian model evaluation using leave-one-out cross-validation and WAIC. *Stat Comput*. 2017;**27**:1413–1432.
  85. Tibshirani R. Regression shrinkage and selection via the lasso. *J Royal Stat Soc Series B*. 1996;**58**(1):267–288. doi: [10.1111/j.2517-6161.1996.tb02080.x](https://doi.org/10.1111/j.2517-6161.1996.tb02080.x)
  86. Buchmann A, Denticò D, Peterson MJ, et al. Reduced mediolateral thalamic volume and prefrontal cortical spindle activity in schizophrenia. *Neuroimage*. 2014;**102 Pt 2**:540–547. doi: [10.1016/j.neuroimage.2014.08.017](https://doi.org/10.1016/j.neuroimage.2014.08.017)
  87. Reinhard MA, Regen W, Baglioni C, et al. The relationship between brain morphology and polysomnography in healthy good sleepers. *PLoS One*. 2014;**9**(10):e109336. doi: [10.1371/journal.pone.0109336](https://doi.org/10.1371/journal.pone.0109336)
  88. Baril A-A, Beiser AS, Mysliwiec V, et al. Slow-wave sleep and MRI markers of brain aging in a community-based sample. *Neurology*. 2021;**96**(10):e1462–e1469. doi: [10.1212/WNL.0000000000011377](https://doi.org/10.1212/WNL.0000000000011377)